

Quantitative Structure–Activity Relationships of 2,4-Diamino-5-(2-X-benzyl)pyrimidines versus Bacterial and Avian Dihydrofolate Reductase†

Cynthia Dias Selassie,* Wei-Xi Gan, Lara S. Kallander, and Teri E. Klein‡

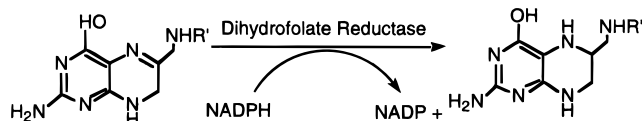
Department of Chemistry, Pomona College, Claremont, California 91711, and Department of Pharmaceutical Chemistry, University of California, San Francisco, California 94143

Received November 14, 1997

Quantitative structure–activity relationships (QSAR) have been formulated for a set of 15 2,4-diamino-5-(2-X-benzyl)pyrimidines versus dihydrofolate reductase from *Lactobacillus casei* and chicken liver. QSARs were also developed for comprehensive data sets containing mono-, di-, and trisubstituted benzyl derivatives. Particular emphasis was placed on the role played by ortho substituents in the overall binding process and subsequent inhibition of the catalytic process in both the prokaryotic and eucaryotic DHFRs. Comparisons between the two QSARs reveal subtle differences at specific positions which can be optimized to design more selective antibacterial agents.

Dihydrofolate reductase (DHFR) catalyzes the reduction of 7,8-dihydrofolate to 5,6,7,8-tetrahydrofolate using NADPH as a cofactor (Scheme 1). Since it wields such

Scheme 1. Reduction of 7,8-Dihydrofolate to 5,6,7,8-Tetrahydrofolate



an important role in the DNA synthetic pathway, its prominence as a target in antibacterial, antiparasitic, and antineoplastic chemotherapy is unsurpassed.¹ In recent years, enhanced structural characterization of various DHFRs from prokaryotic, eucaryotic, and parasitic sources has accelerated the study of various ligand–enzyme interactions as well as the design of selective inhibitors. Relative high homology (75–90%) is found between various vertebrate enzymes unlike bacterial species where homology is around 25–40%. Although the vertebral DHFR enzymes are generally longer (around 25 residues), those insertions are located at various points throughout the sequence and are not clustered in one area. These residues also occur on the protein surface, where they do not appear to affect the overall geometry of the enzyme. Thus, the three-dimensional structures of the vertebrate and bacterial enzymes are similar despite the low degree of homology between them.² Previous efforts from this laboratory have carefully examined the molecular interactions between numerous antifolates and various DHFRs.^{3,4} In a continuation of our study to delineate the intermolecular forces at play in the binding of various inhibitors to DHFR, we have carefully and systematically examined the effects of ortho substitution on the inhibitory potencies of 2,4-diamino-5-(X-benzyl)pyrimidines, **I**.

Earlier studies from our laboratory have focused on the inhibition of chicken liver DHFR and *Lactobacillus casei* DHFR by meta- and para-substituted 2,4-diaminobenzylpyrimidines. Our previous quantitative structure–activity relationship (QSAR) for benzylpyrimidines acting on *L. casei* DHFR is described in eq 1:⁵

$$\log(1/K_i) = 1.24(\pm 0.21)MR_4' + 0.52(\pm 0.27)MR_3' + 0.42(\pm 0.45)MR_5 - 0.13(\pm 0.26)MR^2 + 0.46(\pm 0.21)\pi_4 - 0.92(\pm 0.31)\log(\beta_4 \cdot 10^{\pi_4} + 1) + 0.31(\pm 0.23)\pi_3' - 0.71(\pm 0.36)\log(\beta_3 \cdot 10^{\pi_3'} + 1) + 5.45(\pm 0.17) \quad (1)$$

$$n = 65 \quad r = 0.894 \quad s = 0.245 \quad F_{3,54} = 6.14$$

$$\pi_4^0 = 0.49 \log \beta_4 = -0.501 \log \beta_3 = -1.431$$

$$MR_5^0 = 1.66 \pi_3^0 = 1.33$$

The subscripts 3, 4, and 5 refer to substituents in the meta, para, and other meta positions, respectively. Molecular graphics analysis in tandem with QSAR analyses has established that with certain enzymes, such as DHFR, porcine pancreatic elastase, and papain, the more hydrophobic meta substituent will tend to bind in hydrophobic space placing its counterpart in hydrophilic or aqueous space.⁶ Using selectively ¹³C-enriched trimethoprim, Cheung et al. have also elegantly illustrated the phenomenon of “ring flipping” via two-site exchange between nuclei at the C3' and C5' positions.⁷

Molar refractivity (MR) is often used to quantify steric effects in QSAR studies. It is defined by the Lorentz–Lorenz equation: $MR = (n^2 - 1)/(n^2 + 2)(MW/\delta)$. In this expression, n represents the refractive index, MW is the molecular weight, and δ is the density of the compound. It is thus a crude means of characterizing the bulk and polarizability of a substituent/compound. Although it contains no information on shape, it has found considerable usage in biological QSAR where

†Dedicated to Professor Corwin Hansch on the occasion of his 80th birthday.

‡ University of California.

intermolecular effects predominate. MR is usually scaled by 0.1 to make it equiscalar with π . The prime with MR indicates that the MR term is truncated at a value of 0.79 (the MR value for the methoxy substituent), regardless of the size of the substituent. The occurrence of this feature in the model indicates that beyond a fixed point, the substituents do not effectively contact the enzyme. The positive coefficients of the MR terms suggest that positive steric and/or dispersion effects are operative, thus enhancing the value of $\log(1/K_i)$.

In this model, the steric terms as represented by MR account for approximately 50% of the variance in the data while the other 30% is explained by hydrophobicity. The bilinear model of Kubinyi is used to model the hydrophobic characteristics of the substituents.⁸ The coefficients with both π_3 and π_4 suggest that partial desolvation occurs at the binding site. Despite the presence in the data is explained by the molar refraction terms which suggests that polar/steric interactions are of primary importance in the bacterial enzyme. This result is analogous to what has been observed in the case of DHFR from *Escherichia coli*.⁹ In the 3 and 4 position where any substituent larger than three or two carbon atoms, respectively, encounters interference from the active site residues, the activity falls off dramatically. Hydrophilic substituents in the 5 position have more polar space to maneuver in, around an area that incorporates portions of the sugar moiety of the NADPH cofactor.

Equation 2 was based on the inhibition of chicken liver DHFR by meta- and para-substituted **I**.⁵ Chicken liver DHFR, because of its strong homology with mouse and human DHFR, has been used as a surrogate for the human enzyme.^{10,11}

$$\log(1/K_i) = 0.39\pi_3 + 0.44\pi_4 + 0.37\pi_5 + 0.44\sum\sigma - 0.75MR_5 - 1.04 \log(\beta_3 \cdot 10^{\pi_3} + 1) - 0.32 \log(\beta_4 \cdot 10^{\pi_4} + 1) + 4.70 \quad (2)$$

$$n = 65 \quad r = 0.906 \quad s = 0.207$$

$$\log \beta_3 = -2.69 \quad \log \beta_4 = -0.18 \quad \pi_3^0 = 2.45 \quad \pi_4^0 \cong 3.00$$

The σ (Hammett) term, albeit weak, was perhaps indicative of dipolar interactions between the electron-rich active site of the enzyme and the electron-deficient phenyl ring of the antifolate. The coefficients with π_3 , π_4 , and π_5 suggested that surface binding of these substituents was operative. The steep descending slope with π_3 (-0.65) indicated some obstruction to substituent binding; Val 115 appeared to be the culprit. The flat descending slope with π_4 (-0.10) suggested that hydrophobic substituents larger than a hexyloxy chain in the para position projected beyond the surface into aqueous space. The relatively high negative coefficient with the MR_5 term revealed a constraint to binding in 5-space by large substituents in this area. Tyr 31 with its ability to undergo a conformational change and rotate 180° in the cleft was viewed as the source of this unfavorable interaction.

The two models, although complex in nature, clearly delineated the interactions of the various substituents in the meta and para positions with complementary

sites on the bacterial and avian enzymes. In the present study, 15 new ortho, monosubstituted derivatives of **I** were synthesized, and their inhibitory potencies versus avian and bacterial DHFRs at pH 7.4 were assessed. In addition, five multisubstituted analogues containing substituents in the ortho position were also tested versus these two diverse enzymes.

Results

The following mathematical equations were developed in a stepwise fashion for the inhibition of *L. casei* DHFR at pH 7.20 by ortho-, meta-, and para-substituted 2,4-diamino-5-(X-benzyl)pyrimidines:

$$\log(1/K_i) = 6.68(\pm 0.20) - 0.52(\pm 0.11)B5_6 \quad (3)$$

$$n = 88 \quad r = 0.700 \quad s = 0.545 \quad F_{1,86} = 82.47 \quad q^2 = 0.464$$

$$\log(1/K_i) = 6.12(\pm 0.24) - 0.42(\pm 0.10)B5_6 + 1.00(\pm 0.30)MR'_4 \quad (4)$$

$$n = 88 \quad r = 0.812 \quad s = 0.448 \quad F_{1,85} = 42.54 \quad q^2 = 0.636$$

$$\log(1/K_i) = 5.72(\pm 0.26) - 0.34(\pm 0.09)B5_6 + 1.14(\pm 0.27)MR'_4 + 0.67(\pm 0.28)MR'_3 \quad (5)$$

$$n = 88 \quad r = 0.855 \quad s = 0.400 \quad F_{1,84} = 22.36 \quad q^2 = 0.706$$

$$\log(1/K_i) = 5.57(\pm 0.26) - 0.31(\pm 0.09)B5_6 + 1.11(\pm 0.26)MR'_4 + 0.65(\pm 0.27)MR'_3 + 0.30(\pm 0.16)MR_5 \quad (6)$$

$$n = 88 \quad r = 0.876 \quad s = 0.375 \quad F_{1,83} = 12.88 \quad q^2 = 0.742$$

$$\log(1/K_i) = 5.59(\pm 0.24) - 0.32(\pm 0.08)B5_6 + 1.26(\pm 0.24)MR'_4 + 0.65(\pm 0.24)MR'_3 + 0.28(\pm 0.15)MR_5 + 0.20(\pm 0.18)\pi_4 - 0.84(\pm 0.39) \log(\beta_4 \cdot 10^{\pi_4} + 1) \quad (7)$$

$$n = 88 \quad r = 0.907 \quad s = 0.332 \quad F_{3,80} = 8.47$$

$$q^2 = 0.800 \quad \pi_{4,0} = 0.82(\pm 0.72) \quad \log \beta_4 = -1.338$$

$$\log(1/K_i) = 5.61(\pm 0.23) - 0.32(\pm 0.08)B5_6 + 1.30(\pm 0.24)MR'_4 + 0.62(\pm 0.28)MR'_3 + 0.26(\pm 0.15)MR_5 + 0.21(\pm 0.18)\pi_4 - 0.79(\pm 0.37) \log(\beta_4 \cdot 10^{\pi_4} + 1) + 0.34(\pm 0.30)\pi_3 - 0.65(\pm 0.44) \log(\beta_3 \cdot 10^{\pi_3} + 1) \quad (8)$$

$$n = 88 \quad r = 0.918 \quad s = 0.319 \quad F_{3,77} = 3.31$$

$$q^2 = 0.816 \quad \pi_{4,0} = 0.71(\pm 0.92) \quad \log \beta_4 = -1.159$$

$$\pi_{3,0} = 1.10(\pm 0.76) \quad \log \beta_3 = -1.057$$

$$\begin{aligned} \log(1/K_i) = & 5.87(\pm 0.30) - 0.27(\pm 0.12)B5_6 + 1.28(\pm 0.22)MR'_4 + \\ & 0.64(\pm 0.27)MR'_3 + 0.27(\pm 0.14)MR_5 + \\ & 0.17(\pm 0.16)\pi_4 - 0.78(\pm 0.36) \log(\beta_4 \cdot 10^{\pi_4} + 1) + \\ & 0.34(\pm 0.29)\pi_3 - 0.65(\pm 0.42) \log(\beta_3 \cdot 10^{\pi_3} + 1) + \\ & 0.84(\pm 0.62)\pi_6 - 1.02(\pm 0.95) \log(\beta_6 \cdot 10^{\pi_6} + 1) \quad (9) \\ n = 88 \quad r = 0.929 \quad s = 0.304 \quad F_{3,74} = 3.59 \\ q^2 = 0.821 \quad \pi_{4,0} = 0.78(\pm 0.96) \log \beta_4 = -1.354 \\ \pi_{3,0} = 1.09(\pm 0.76) \log \beta_3 = -1.037 \\ \pi_{6,0} = 0.66(\pm 0.85) \log \beta_6 = 0.032 \end{aligned}$$

In these equations, n represents the number of data points, r is the correlation coefficient, q^2 is the cross-validated r^2 , and s is the standard deviation from the regression. F represents the F statistic for the significance of each added variable. A sterimol parameter, $B5$, is used for the first time with these compounds.¹² $B5$ is defined as a maximum-width parameter. It represents a rough approximation since in the case of unsymmetrical substituents, $B5$ can be defined in a few different ways. As in our previous work, the more hydrophobic meta substituent is placed in the 3 position, while its more hydrophilic meta counterpart is located in the 5 position. In the case of the ortho-substituted **I**, these were mostly classified as being in the 6 position where binding was favored over the 2 position as delineated by a more favorable r and substantiated by molecular graphics analysis. Exceptions to this rule were the 2,3- Cl_2 and 2,3-(OCH_3)₃ analogues. Placing them in 6,5-space led to a slightly poorer overall correlation for eq 9 ($r = 0.920$, $s = 0.323$). More than that, they were outliers whose inhibitory activity was off by 0.69 (2,3-(OCH_3)₂) and 0.67 (2,3- Cl_2). Interestingly, the activity of the former analogue (5.92) was very similar to that of the 3- OCH_3 (5.88), while the activity of the latter analogue (6.37) was around that of the 3- Cl analogue (5.90). This behavior suggested that the slight hydrophobicity of the 3-*m*-methoxy group (0.02) in 2,3-(OCH_3)₃ and the pronounced hydrophobicity of the *m*-chloro (0.61) in 2,3- Cl_2 analogues warranted their placement in hydrophobic 3-space. Thus, the ortho groups of these two analogues were forced into restricted 2-space unlike the other ortho-substituted **I**. With pseudo-TMP (2,3,4-(OCH_3)₃) this would not occur because the hydrophilic methoxy group in the meta position would favor binding in hydrophilic 5-space. (See section on Molecular Graphics Analysis.)

The MR terms represent the bulk of the substituents in the individual ortho, meta, or para positions. The MR terms in the 3 and 4 positions are truncated at a value of 0.79 which corresponds to the value of a methoxy group, since earlier studies indicated that substituents larger than a methoxy group did not enhance binding to the receptor. The hydrophobicities of the substituents in the 3, 4, and 6 positions are represented by π_3 , π_4 , and π_6 , respectively. With the bacterial enzyme, 80% of the variance in the data can be explained by steric terms. In the 3, 4, and 5 positions the presence of a bulky polarizable substituent tends to enhance inhibitory potency, while the width of the substituent in the ortho position appears to hinder

binding. Equation 3 suggests that the presence of any substituent in the ortho position that is not small is detrimental to overall binding in the bacterial enzyme. Overall hydrophobicity of the substituents in the combined data set only accounts for 10% of the variance in the data. These results once again establish the importance of polarity and/or steric effects in the interactions of this class of antifolates with the bacterial enzyme. Equations 3–9 are all significant at the 95% level. Two points were not particularly well-predicted in the final analysis; they were the 4-OH and 2-OH derivatives which were underpredicted and overpredicted, respectively. Excluding them from the analysis resulted in the formulation of a slightly more rigorous equation with the following statistics: $n = 86$, $r = 0.970$, $q^2 = 0.853$, $s = 0.272$.

The low coefficients with the hydrophobic terms in eq 9 suggest that partial desolvation of the substituents occurs at the enzyme surface. In the 3, 4, and 6 positions the optimum hydrophobicities (1.09, 0.78, and 0.66, respectively) are also relatively low which indicates that added hydrophobicity beyond those cutoff values results in a pronounced drop in inhibitory activity. This is particularly apparent in the para position where the descending slope of the bilinear equation is substantial ($0.78 - 0.17 = 0.61$); with moderately hydrophobic substituents, the negative impact of hydrophobicity is offset by the large positive contribution (+1.28) of the steric term as represented by MR'_4 .

The two points that were not well-predicted in the analysis, 4-OH and 2-OH, were off by more than two standard deviations. The 2-OH derivative was 4 times less active than predicted, while the 4-OH was underpredicted by a factor of 7. The anomalous behavior of the 2-OH analogue cannot be attributed to lack of hydrophobicity. It has been suggested that the phenolic hydroxy group may alter the positioning of the cofactor and subsequently affect catalysis.¹³ Its placement in 6-space would place it in close proximity to the ribose moiety of the cofactor. It is of interest to note that the 3-OH derivative is well-fit and falls within the standard deviation of the equation.

An examination of the ortho-monosubstituted analogues as a separate subset (Table 1) resulted in the development of eqs 10 and 11. The 2-hydroxy analogue was not included in the analysis.

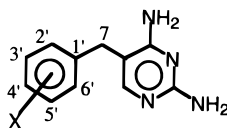
$$\log(1/K_i) = 5.42(\pm 0.32) - 0.23(\pm 0.09)B5_6 \quad (10)$$

$$n = 15 \quad r = 0.827 \quad s = 0.229 \quad F_{1,13} = 28.02 \quad q^2 = 0.607$$

$$\begin{aligned} \log(1/K_i) = & 5.30(\pm 0.21) + 0.50(\pm 0.23)\pi_6 - \\ & 0.81(\pm 0.46) \log(\beta_6 \cdot 10^{\pi_6} + 1) - 0.15(\pm 0.08)B5_6 \quad (11) \end{aligned}$$

$$\begin{aligned} n = 15 \quad r = 0.958 \quad s = 0.133 \quad F_{2,10} = 9.46 \\ q^2 = 0.824 \quad \pi_{6,0} = 0.78(\pm 0.58) \log \beta_6 = -0.559 \end{aligned}$$

Both eqs 10 and 11 are significant at the 99% level. Approximately 70% of the variance in the monosubstituted ortho derivatives can be handled by the steric term, while about 20% of the variance is defined by the hydrophobic term. This is slightly higher than the value obtained for the rest of the benzylpyridines (10%).

Table 1. Physicochemical Parameters of 2,4-Diamino-5-(X-benzyl)pyrimidines **I** Used in the Derivation of Eqs 11 and 21

X	log(K_i)				SI $\Delta\log(1/K_i)$ calcd ^c	physicochemical parameters			
	chicken DHFR		<i>L. casei</i> DHFR			$\pi_{2(6)}$	B ₅₆	MR ₂	σ
	obsd	pred ^a	obsd	pred ^b					
2-H	4.71	4.48	5.20	5.06	0.49	0	1.00	0.1	0
2-F	4.36	4.53	5.02	5.05	0.66	0.14	1.35	0.09	0.06
2-Cl	4.76	4.77	5.02	5.08	0.26	0.71	1.80	0.60	0.23
2-Br	4.91	4.83	5.00	5.05	0.09	0.86	1.95	0.88	0.23
2-I	5.06	4.93	4.94	5.00	-0.12	1.12	2.15	1.39	0.18
2-CH ₃	4.53	4.57	5.02	5.03	0.49	0.56	2.04	0.57	-0.17
2-CH ₂ OCH ₃	4.40	4.63	4.55	4.69	0.15	-0.03	3.40	1.21	0.03
2-OSO ₂ CH ₃	4.64	4.69	4.07	4.23	-0.57	-0.87	4.10	1.70	0.36
2-OCH ₂ CONH ₂	4.47	4.30	4.10	4.00	-0.37	-1.37	3.98	1.60	-0.33
2-OH	4.05	4.26	3.96	4.65	-0.09	-0.67	1.93	0.29	-0.37
2-OCH ₃	4.54	4.48	5.00	4.80	0.46	0.17	3.07	0.79	-0.27
2-OCH ₂ CH ₃	4.61	4.60	4.70	4.80	0.09	0.38	3.36	1.25	-0.24
2-OCH ₂ CH=CH ₂	4.67	4.72	4.87	4.68	0.20	0.81	4.42	1.62	-0.25
2-O(CH ₂) ₃ CH ₃	5.06	4.89	4.45	5.52	-0.61	1.55	4.79	2.17	-0.32
2-O(CH ₂) ₅ CH ₃	5.10	5.20	4.00	3.99	-1.10	2.67	6.23	3.07	-0.34
2-OCH ₂ C ₆ H ₅	5.04	5.08	4.74	4.69	-0.30	1.66	3.50	3.17	-0.23

^a Predicted using eq 21. ^b Predicted using eq 11. ^c Selectivity index = observed $\log(1/K_i)$ (*L. casei* DHFR) - $\log(1/K_i)$ (chicken liver DHFR).

Nevertheless, it is apparent that binding space is also restricted in the 6 position and that substituents with a wide girth are not conducive to effective binding in this area. The activity of the 2-hydroxy analogue was overpredicted by a factor of 5.

The results for the inhibition of chicken liver DHFR by **I** are delineated in the following equations:

$$\log(1/K_i) = 4.53(\pm 0.08) + 0.40(\pm 0.15)\pi_3 - 1.12(\pm 0.75) \log(\beta_3 \cdot 10^{\pi_3} + 1) \quad (12)$$

$$n = 85 \quad r = 0.533 \quad s = 0.377 \quad F_{3,81} = 10.72 \\ q^2 = 0.229 \quad \pi_{3,0} = 2.48(\pm 0.93) \quad \log \beta_3 = -2.735$$

$$\log(1/K_i) = 4.67(\pm 0.09) + 0.47(\pm 0.13)\pi_3 - 1.13(\pm 0.51) \log(\beta_3 \cdot 10^{\pi_3} + 1) - 0.60(\pm 0.21)MR_5 \quad (13)$$

$$n = 85 \quad r = 0.695 \quad s = 0.322 \quad F_{1,80} = 30.76 \\ q^2 = 0.434 \quad \pi_{3,0} = 2.26(\pm 1.04) \quad \log \beta_3 = -2.397$$

$$\log(1/K_i) = 4.82(\pm 0.12) + 0.45(\pm 0.11)\pi_3 - 1.11(\pm 0.44) \log(\beta_3 \cdot 10^{\pi_3} + 1) - 0.63(\pm 0.18)MR_5 + 0.60(\pm 0.25)\pi_4 - 0.59(\pm 0.33) \log(\beta_4 \cdot 10^{\pi_4} + 1) \quad (14)$$

$$n = 85 \quad r = 0.808 \quad s = 0.269 \quad F_{3,77} = 12.54 \\ q^2 = 0.593 \quad \pi_{3,0} = 2.28(\pm 0.95) \quad \log \beta_3 = -2.442 \\ \pi_{4,0} = \sim 3.0 \quad \log \beta_4 = -0.215$$

$$\log(1/K_i) = 4.73(\pm 0.10) + 0.45(\pm 0.10)\pi_3 - 1.14(\pm 0.42) \log(\beta_3 \cdot 10^{\pi_3} + 1) - 0.59(\pm 0.16)MR_5 + 0.53(\pm 0.21)\pi_4 - 0.49(\pm 0.29) \log(\beta_4 \cdot 10^{\pi_4} + 1) + 0.24(\pm 0.11)\pi_2 \quad (15)$$

$$n = 85 \quad r = 0.849 \quad s = 0.243 \quad F_{1,76} = 18.37 \\ q^2 = 0.659 \quad \pi_{3,0} = 2.34(\pm 0.84) \quad \log \beta_3 = -2.529 \\ \pi_{4,0} = \sim 3.0 \quad \log \beta_4 = -0.302$$

$$\log(1/K_i) = 4.74(\pm 0.10) + 0.43(\pm 0.09)\pi_3 - 1.07(\pm 0.39) \log(\beta_3 \cdot 10^{\pi_3} + 1) - 0.66(\pm 0.15)MR_5 + 0.50(\pm 0.21)\pi_4 - 0.43(\pm 0.28) \log(\beta_4 \cdot 10^{\pi_4} + 1) + 0.26(\pm 0.10)\pi_2 + 0.32(\pm 0.17)\Sigma\sigma \quad (16)$$

$$n = 85 \quad r = 0.874 \quad s = 0.225 \quad F_{1,75} = 13.91 \\ q^2 = 0.708 \quad \pi_{3,0} = 2.35(\pm 0.91) \quad \log \beta_3 = -2.522 \\ \pi_{4,0} = \sim 3.0 \quad \log \beta_4 = -0.218$$

$$\log(1/K_i) = 4.77(\pm 0.11) + 0.39(\pm 0.09)\pi_3 - 1.03(\pm 0.43) \log(\beta_3 \cdot 10^{\pi_3} + 1) - 0.76(\pm 0.17)MR_5 + 0.52(\pm 0.21)\pi_4 - 0.43(\pm 0.28) \log(\beta_4 \cdot 10^{\pi_4} + 1) + 0.26(\pm 0.10)\pi_2 + 0.34(\pm 0.16)\Sigma\sigma + 0.38(\pm 0.30)\pi_5 \quad (17)$$

$$n = 85 \quad r = 0.885 \quad s = 0.217 \quad F_{1,74} = 6.24 \\ q^2 = 0.723 \quad \pi_{3,0} = 2.42(\pm 0.89) \quad \log \beta_3 = -2.646 \\ \pi_{4,0} = \sim 3.0 \quad \log \beta_4 = -0.132$$

$$\log(1/K_i) = 4.68(\pm 0.10) + 0.39(\pm 0.09)\pi_3 - \\ 1.05(\pm 0.43) \log(\beta_3 \cdot 10^{\pi_3} + 1) - 0.74(\pm 0.17)MR_5 + \\ 0.44(\pm 0.19)\pi_4 - 0.34(\pm 0.26) \log(\beta_4 \cdot 10^{\pi_4} + 1) + \\ 0.17(\pm 0.13)\pi_2 + 0.38(\pm 0.16)\Sigma\sigma + 0.37(\pm 0.29)\pi_5 + \\ 0.11(\pm 0.10)MR_2 \quad (18)$$

$$n = 85 \quad r = 0.892 \quad s = 0.212 \quad F_{1,73} = 4.62 \\ q^2 = 0.737 \quad \pi_{3,0} = 2.46(\pm 0.85) \quad \log \beta_3 = -2.687 \\ \pi_{4,0} = \sim 3.00 \quad \log \beta_4 = -0.331$$

Treatment of mono-ortho-substituted **I** as a subset leads to the development of the following equations with respect to the inhibition of chicken liver DHFR. (See Table 1.)

$$\log(1/K_i) = 4.57(\pm 0.11) + 0.23(\pm 0.10)\pi_2 \quad (19)$$

$$n = 16 \quad r = 0.785 \quad s = 0.191 \quad F_{1,14} = 22.44 \quad q^2 = 0.473$$

$$\log(1/K_i) = 4.59(\pm 0.11) + 0.24(\pm 0.10)\pi_2 + \\ 0.32(\pm 0.42)\Sigma\sigma \quad (20)$$

$$n = 16 \quad r = 0.825 \quad s = 0.180 \quad F_{1,13} = 2.64 \quad q^2 = 0.428$$

$$\log(1/K_i) = 4.46(\pm 0.15) + 0.18(\pm 0.10)\pi_2 + \\ 0.14(\pm 0.11)MR_2 + 0.43(\pm 0.37)\Sigma\sigma \quad (21)$$

$$n = 16 \quad r = 0.891 \quad s = 0.151 \quad F_{1,12} = 6.66 \quad q^2 = 0.594$$

Equation 18 is very similar to eq 2 with the exception of the inclusion of the parameters for the ortho position. The coefficients of the various π terms (0.38 (π_3), 0.45 (π_4), and 0.38 (π_5)) establish the hydrophobic homogeneity of the binding site and also indicate that partial desolvation of the substituents provides the driving force for these interactions. Using free energy simulation methods, Fleischman and Brooks and McDonald and Brooks have also concluded that entropic contributions and desolvation thermodynamics play a critical role in overall binding to the avian enzyme.^{14,15} The similarity in the values, in particular, the two meta positions and the para positions, suggests that these terms could be incorporated into one parameter (π_{345}) as was done in one of our earlier studies.¹⁶ However this would be misleading as the downward slope of the bilinear equation in the 3 and 4 positions differs drastically and the 5 position only calls for a linear dependence on hydrophobicity. The strong negative slope in the 3 position ($1.04 - 0.38 = 0.66$) is suggestive of either steric hindrance encountered by a 3-substituent which may be protruding into a bulky residue or a change in the hydrophobic characteristics of the binding site beyond five carbon atoms. The negative dependence on bulk as denoted by the negative coefficient of the MR_5 term indicates that some amino acid residue presents a strong deterrent to binding in this general vicinity. This positioning also has an effect on the ortho-substituted analogues which are all forced into the 2 position irrespective of hydrophobicity or size. The coefficient with the hydrophobic term in the 2 position is very small and suggests that the ortho substituents barely make hydrophobic contact with the enzyme. Indeed the

variation in the inhibitory activity of the ortho-substituted derivatives only extends from 4.03 to 5.06, despite a range of 4 log units in hydrophobicity.

Three data points were not included in the analysis. The omitted compounds were the 3,4,5-(CH_2CH_3)₃, 3-OH, and 4-OCF₃ analogues. The first analogue was approximately 4 times more active than predicted, while the latter two were overpredicted by a factor of 4. In the case of the 3,4,5-triethyl analogue which is an isostere of trimethoprim, the low predicted activity may be attributed to inadequate parametrization of the hydrophobic contributions of each of the ethyl groups. The partition coefficient of the molecule has been measured, and the sum of the substituents' hydrophobicity is deemed to be about 2.58; the contribution for each ethyl group is ascertained to be the same at a value of 0.86. Steric crowding around the *p*-ethyl substituent subsequently alters its solvation by water, resulting in unequal solvation of the adjacent ethyl groups. The *p*-ethyl substituent would tend to be more hydrophilic than the adjacent *m*-ethyl groups since it would be forced out of the plane of the benzene ring. Greater assignment of the hydrophobic contribution to the meta positions would thus enhance the predictive inhibitory activity of the 3,4,5-triethyl **I**.

An analysis of the mono-ortho-substituted **I** reveals a similar dependence on hydrophobicity, size, and electronic character of the substituents. Hydrophobicity alone accounts for 62% of the variance in the data, while $\Sigma\sigma$ only accounts for 6% of the variance in the data. The 95% confidence interval is also rather high. Further inclusion of the MR_2 term in eq 21 is significant at the 95% level of confidence as delineated by the *F* statistic. The 95% confidence interval on the σ term is still high but less than the coefficient of the electronic term. The inadequacy of spanned space with regard to the σ parameter (0.6) is responsible for the high confidence intervals in eqs 20 and 21. It is of interest to note that in the comprehensive data set, spanned space in $\sigma = 1.61$ and the confidence interval is quite satisfactory.

Molecular Graphics Analysis of the Binding of 2,4-Diamino-5-(2',3',4'-trimethoxybenzyl)pyrimidine (Pseudo-TMP) to Chicken Liver DHFR and *L. casei* DHFR. The molecular models of the binding of avian and bacterial DHFR–benzylpyrimidine complexes have been previously described.³ The structures of pseudo-TMP **88** were generated using the program LeAP from the Amber suite of programs.¹⁷ The inhibitors were minimized in LeAP and then least-squared fit to the inhibitors in the original crystallographic structures. The solvent-accessible surface was calculated using the program dms contained in the UCSF Midas Plus suite of programs. These images were created using the program Neon contained in Midas Plus.¹⁸ Hydrophobic surfaces are colored red, semihydrophobic surfaces are colored yellow, and hydrophilic surfaces are visualized in blue.

1. Binding to *L. casei* DHFR (Figure 1). The benzyl side chain and its attendant phenyl ring avoid coplanarity with the pyrimidine ring and are in a perpendicular juxtaposition to it. It is also positioned lower down in the active site pocket and oriented toward the nicotinamide binding site. The binding area available to a substituent in the 2 position of the benzyl ring

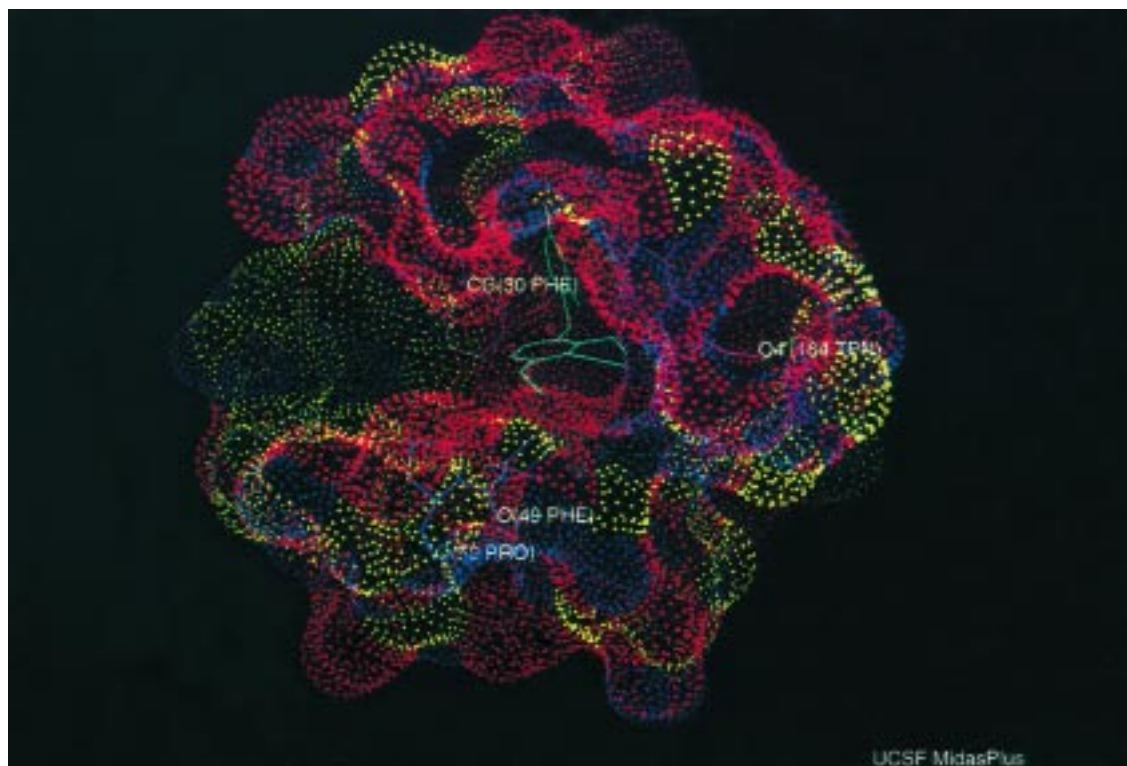


Figure 1. Binding of pseudo-TMP to *L. casei* DHFR.

is constricted and limited by the presence of Phe 30. More than that, there is also a steric interaction between the C1' and C2' carbons and the H6 proton which are in close van der Waals contact due to the folded conformation adopted by the analogue when bound to the enzyme. A 180° rotation of the benzyl ring about the C7–C1' bond places the methoxy substituent in 6-space which is more extensive and hydrophilic and away from the side chain of Leu 27 in 3-space. The low optimum π_6 (0.59) suggests that the binding area is marginally hydrophilic and that desolvation of the ortho substituent is limited such that binding occurs on the surface. The weak negative coefficient of the B5₆ term suggests that the binding of substituents with substantial width is ill-favored in this region, which is defined in part by the surface of the 2'-hydroxyl of the coenzyme NADP. The methoxy substituent in the meta position is also exposed to this hydrophilic surface where enhanced dispersion interactions occur as expressed by the positive coefficient with the MR₅ term. The methoxy group in the 4 position is partially desolvated in this extensive flat hydrophilic milieu delineated by residues Ser 48, Phe 49, Pro 50, and Leu 19. Buttressing of the 4-substituent up against the Pro 50 residue results in a substantial drop in activity with increasing hydrophobicity (i.e., beyond 0.8 unit).

2. Binding to Chicken Liver DHFR (Figure 2).

This model was constructed based on the X-ray crystallography coordinates of the ternary complex of trimethoprim–DHFR–NADPH.¹⁹ The active site of chicken liver DHFR is much wider than that in the *E. coli* enzyme by approximately 1.5–2.0 Å. Overall it is also much more hydrophobic and extensive. The inhibitor is inserted deeper into the active site of this enzyme and binds with a butterfly-type conformation. The *o*-methoxy group binds in what is designated as 2-space as opposed to 6-space which is crowded by the bulk of Tyr

31. 2-Space is defined as a narrow cleft between the methylene bridge of the benzyl ring and the NADPH cofactor; the methoxy substituent is buttressed up against the C4–C5–C6 edge of the nicotinamide moiety of the cofactor, hence the weak positive coefficient with both the MR₂ term and the hydrophobic π_2 parameter. 5-Space and 6-space are highly constricted by the presence of Tyr 31, and the positioning of this residue precludes binding in this general vicinity; substantial steric hindrance in this area is denoted by the strong, negative MR₅ term. The 3- and 4-methoxy groups are partially desolvated by an extensive hydrophobic surface which is comprised of six hydrophobic residues: Phe 34, Met 52, Ile 60, Leu 67, Val 115, and the side chain of Thr 56. Val 115 is a strong deterrent to binding in the 3 position; the steep descending slope of the bilinear equation is testament to its negative impact on binding.

Discussion

The pyrimidine ring binds in a manner similar to DHFR from both bacterial and avian species, with the exception of a loss of a hydrogen bond between N4 of the pyrimidine ring and the carbonyl group of Val 115 in the chicken liver complex. It is clear however that the benzyl moiety lies in different environments in the ternary complexes; in the *L. casei* complex, this moiety projects beyond the binding site and toward the area occupied by the cofactor, while in the chicken liver complex, with the butterfly arrangement of I, the potential for favorable van der Waals contacts is much greater.

According to eq 9, it is clear that 2–3-binding space is not equivalent to 6–5-binding space, in terms of hydrophobicity and steric constraints. The ability of the 2,4-diamino-5-(X-benzyl)pyrimidines to undergo a 180° rotation about the C7–C1' bond in order to place the substituents in a more favorable binding environment

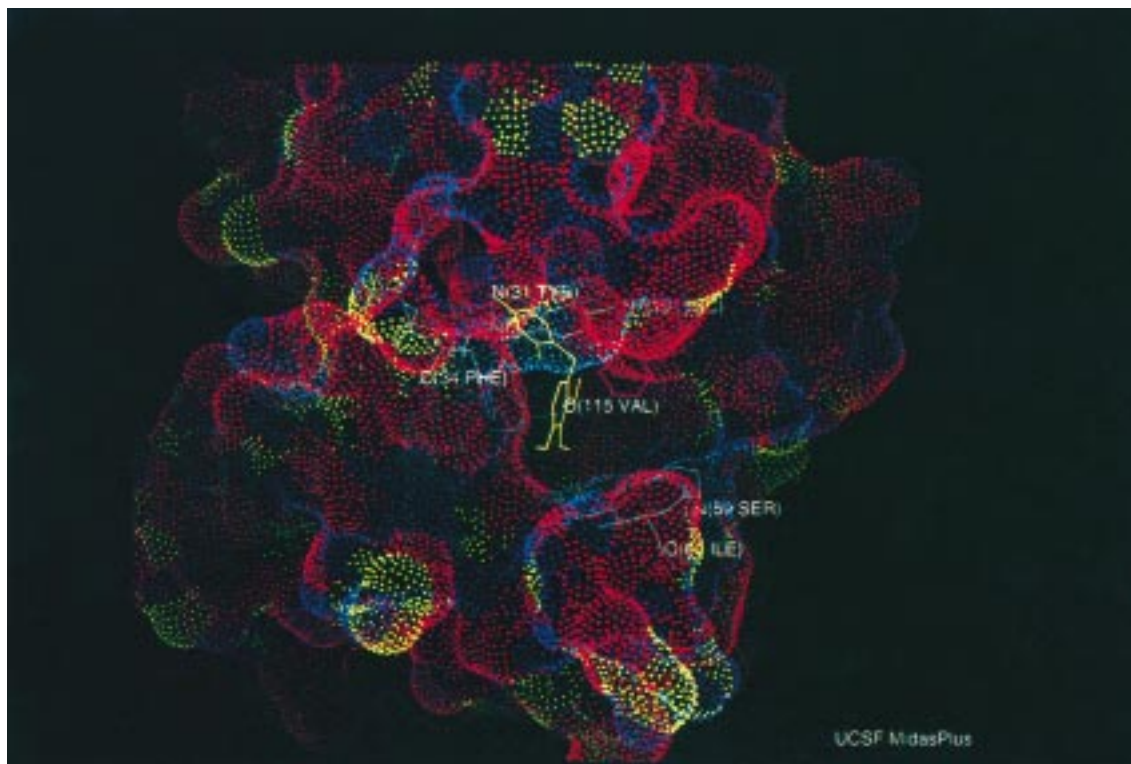


Figure 2. Binding of pseudo-TMP to chicken liver DHFR.

is well-documented. The phenomenon of “ring flipping” has been well-established by ^{13}C NMR studies of the binding of trimethoprim to *L. casei* DHFR.^{7,20,21} Recent EPR studies on spin-labeled inhibitors in *L. casei* DHFR substantiate these results.²² In the case of monosubstituted analogues, “ring-flipping” places all the substituents in the more accessible 6-space. With multisubstituted analogues, e.g., 2,3-dichloro analogue, the situation is complex. While the ortho substituent would favor 6-space, the meta substituents would have a tendency to bind in the more hydrophobic 3-space. The drive to desolvate the substituents in hydrophobic 3-space overrides all other constraints and favors the localization of the two hydrophobic chloro groups in 2,3-space, despite the steric hindrance in 2-space. Using this assumption, the activity of the analogue is well-predicted and its standard deviation is well within the average deviation for the whole set. Thus the overall assignment of hydrophilic meta and all ortho substituents to 5–6-space and hydrophobic meta substituents to 3-space results in a better correlation and a more cohesive and consistent model.

Equations 9 and 18 pertaining to the inhibition of *L. casei* and chicken liver DHFR, respectively, are complex and multifaceted equations which serve to pinpoint regularities in behavior of the ortho, meta, and para substituents. These positional isomers vary considerably in their interactions with both the avian and bacterial enzymes as can be vividly illustrated in the case of the monomethoxy-substituted I. (See Table 2.) In the more hydrophobic avian enzyme, as one moves from the ortho to the para derivatives, the inhibitory activity drops slightly ($\Delta K_i = 0.15$), while the reverse ($\Delta K_i = 1.25$) is seen in the case of the more hydrophilic bacterial enzyme. It is clear from these models that substitution in the ortho position, while favorable to binding in the avian enzyme, is not conducive to binding

Table 2. Comparison of Activities of Equilipophilic 2,4-Diamino-5-(X-benzyl)pyrimidines I

X	log(1/C)		$\Delta\log(1/K_i)$ SI ^a
	chicken DHFR	<i>L. casei</i> DHFR	
2-OCH ₃	4.54	5.00	0.46
3-OCH ₃	4.45	5.93	1.48
4-OCH ₃	4.29	6.25	1.96
2,3,4-(OCH ₃) ₃ (pseudo-TMP)	4.79	6.22	1.43
3,4,5-(OCH ₃) ₃ (TMP)	3.98	6.88	2.90

^a SI = $\log(1/K_i(L. casei \text{ DHFR})) - \log(1/K_i(\text{chicken liver DHFR}))$.

to the bacterial enzyme. The avian enzyme has often been used as a surrogate for human DHFR since the two enzymes are highly homologous with no insertions or deletions. It is thus assumed that they have a similar backbone structure. Recently it has been shown that the mouse L1210 enzyme also falls into the same general class.²³

The detrimental behavior of the ortho substituent toward the *L. casei* enzyme has also been seen versus *E. coli* dihydrofolate reductase. Stuart et al. evaluated the binding characteristics of pseudo-TMP versus *E. coli* and rat liver DHFR.¹³ Calculated $\log(1/K_i)$ values of TMP versus *E. coli* and rat liver DHFR were 8.15 and 3.50, respectively, while pseudo-TMP yielded values of 6.03 and 4.20 versus *E. coli* and rat liver DHFR, respectively. It is assumed that pseudo-TMP will also undergo 180° flipping in the case of the *E. coli* bacterial enzyme which would place the methoxy groups in the 4, 5, and 6 positions. The steric hindrance encountered

in 6-space likely hinders maximal binding of this analogue to *E. coli* DHFR.

Some of this steric hindrance may be attributed to the topography of the methoxy-substituted benzene ring. It is well-established that the 3,5-dimethoxy groups of TMP lie mainly in the plane of the benzene ring away from the methoxy group at C4' of TMP which lies out of plane.²⁴ In the case of pseudo-TMP, Stuart et al. indicate that vicinal substituents on either side force the 2(6)- and 3(5)-methoxy groups out of plane in opposite directions thus allowing the 4-methoxy group to attain planarity with the ring but away from the 3-substituent.¹³ X-ray crystallographic analysis of tetramethoprim ($X = 3,4,5,6-(\text{OCH}_3)_4$) and pentamethoprim ($X = 2,3,4,5,6-(\text{OCH}_3)_5$) indicated that out-of-plane methoxy groups predominate in these analogues.²⁵ In tetramethoprim only the 5-methoxy is coplanar with the benzene ring, while the other methoxy groups are rotated down, up, and up with respect to the phenyl plane. In pentamethoprim, the methyl groups of the five methoxy groups are alternately oriented down, up, down, up, down. Thus the topography of the methoxy-substituted analogues is such that TMP has one methyl group protruding out of the plane, and pseudo-TMP has two, while tetramethoprim and pentamethoprim have three and five, respectively. The latter two compounds were not assayed versus any bacterial DHFR, but bacteriological screening indicated that TMP was at least 10 times more active versus *E. coli* cultures than tetramethoprim while pentamethoprim was ineffective. As suggested by the strong dependence on MR terms in eq 9, polar/dispersive interactions in the meta and para positions are of critical importance in the overall response to the bacterial enzyme. Exposure of the polar oxygen atoms to the hydrophilic milieu in the *L. casei* enzyme without shielding by the methyl groups enhances overall binding. Also substituents in the ortho position with enhanced width have a deleterious effect on binding. Note that TMP has no ortho substituents. Pseudo-TMP and tetramethoprim both have one each, while Pentamethoprim has two.

Roth et al. also examined the effects of total substitution on the ring by analyzing the binding characteristics of two symmetrical I analogues, 2,3,5,6-tetramethyl-4-methoxy and 2,3,5,6-tetramethyl-4-ethoxy, again versus *E. coli* DHFR.²⁶ For the 4-methoxy and 4-ethoxy methylated analogues, activities of 6.50 and 6.42 were obtained. Note that 3,5-dimethyl-4-methoxy had a log($1/C$) value equal to 6.82. Obviously substitution in both the ortho positions caused a significant (0.32) drop in activity. The activities of the tetramethyl compounds were also assessed versus rat liver DHFR. Unfortunately test concentrations higher than the micromolar level were not utilized; no inhibition was apparent at this low concentration. However the 3,5-dimethyl-4-methoxy analogue did yield an activity of approximately 3.60, and it is conceivable that the tetramethyl analogues would lie within 1 log unit since the 3,5-diethyl-4-methoxy analogue yields a value of 4.24. The selectivity indices, which are the ratios of the antibacterial activities to antimammalian activities, would be low (2.30) compared to that of TMP (8.15 - 3.50 = 4.65).

Chan and Roth in an elegant study designed and evaluated a conformationally restricted analogue of

TMP:²⁷ 2,3-dihydro-1-(2,4-diamino-5-pyrimidyl)-1*H*-indene, which would certainly preclude ring flipping. Versus *E. coli* and rat liver DHFR, the following log($1/C$) values were obtained respectively: 5.85 and 3.39. The selectivity index was 2.46 which again substantially deviates from that of TMP. Its similar activity to TMP versus the rat enzyme suggests that it can adopt a similar mode of binding. However, versus the *E. coli* enzyme, the constrained analogue does not allow rotation about the C7-C1' bond as seen in Figure 2, and thus the analogue is forced to adopt the unfavorable conformation in 2-space and not 6-space which most of the flexible analogues favor.

Conclusion

On the basis of the preceding analysis, we offer the following generalizations. The type and positioning of the substituent on the benzyl ring of the inhibitor nucleus clearly determines the selectivity of the analogue. Within the binding site, the region available to the ortho and meta substituents in both the bacterial and avian enzyme is clearly not equivalent. Rotation or "flipping" about the C1'-C7 bond to maximize van der Waals interactions at the molecular level is prevalent particularly in nonequivalent monosubstituted or disubstituted analogues. Thus careful analysis via the QSAR paradigm is useful in revealing anomalies in binding behavior. A case in point was illustrated by the 2,3-Cl₂ and 2,3-dimethoxy analogues where desolvation of the substituents was of overriding importance in binding and overruled steric constraints in these particular cases.

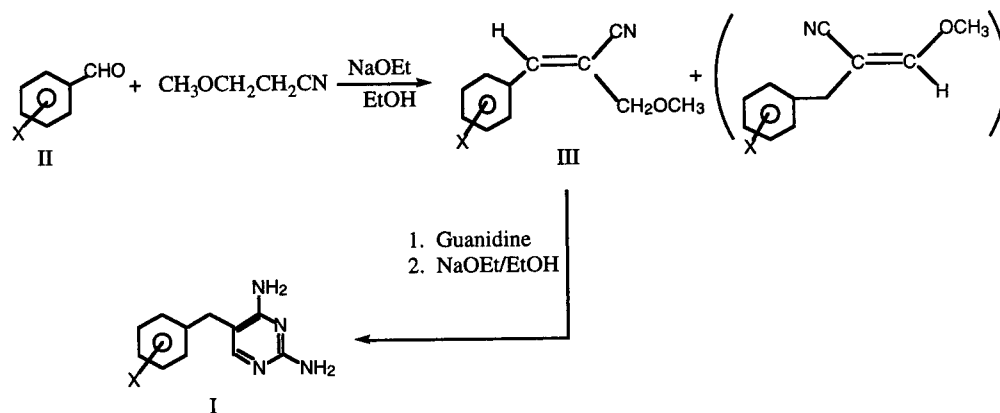
From the drug design perspective, the presence of ortho substituents does little to enhance selectivity in these 2,4-diamino-5-(X-benzyl)pyrimidines. In the case of the ortho-monosubstituted analogues, it is clear that the lack of large, hydrophilic substituents in the 4,5 position and a moderate hydrophobic moiety in the 3 position severely curtails their antifolate activity. Preliminary work with a carefully designed series of non-symmetrical trisubstituted analogues shows promising activity against *E. coli* DHFR and weak activity versus avian DHFR.²⁸ The specificity of DHFRs from various bacterial and mammalian sources has been critically examined using different tools and approaches for the last 30 years. Nevertheless the flexibility of the binding sites in the proteins continues to reveal subtle nuances in behavior with each new ligand probe. Roberts has aptly stated that "the conformational flexibility of proteins and the subtlety of their responses to amino-acid substitutions and changes in ligand structure continue to present substantial challenges".²⁹

Experimental Section

QSAR Analysis. The π constants for most of these substituents are well-documented.³⁰ The partition coefficients of many of the benzylpyrimidines have been previously measured. Some partition coefficients are measured, and their π values are calculated. The multiregression analysis was done by using the C-QSAR suite of programs (BioByte, Inc.).

Enzyme Studies. DHFR from *L. casei* was purchased from Biopure Fine Chemicals, Inc. (Boston, MA) as a lyophilized powder. It was dissolved in 0.05 M Tris buffer, pH 7.20, to yield approximately 0.5 enzyme unit/mL. Aliquots were stored at -20 °C and were thawed just before using. The buffer contained 50 mM mercaptoethanol to prevent oxidation. The

Scheme 2. Synthesis of 2,4-Diamino-5-(X-benzyl)pyrimidines I



solutions of dihydrofolic acid (FAH₂) and NADPH were kept at 0 °C. The benzylpyrimidines were solubilized with DMSO such that the final concentration of DMSO did not exceed 0.5%. DHFR activity with and without added inhibitor was determined by the standard spectrophotometric assay which monitors the oxidation of NADPH to NADP⁺ and the concomitant reduction of FAH₂ to FAH₄ at 340 nm by using a stopped flow spectrophotometer. The *K_i*, log(1/*K_i*), and 95% confidence limits were determined by using the jackknife procedure.³¹

DHFR from chicken liver was a generous gift from B. T. Kaufman (NIADDK, NIH, Bethesda, MD). Each vial contained 0.19 enzyme unit/mL. Each vial was dissolved in 24 mL of 200 μM NADPH and used as previously described.³¹

Synthesis. Melting points were determined with a Buchi melting point apparatus and are uncorrected. IR and NMR spectra are in agreement with the structures cited and were recorded on a Perkin-Elmer 12 or a Perkin-Elmer FTIR 1600 and a GE QE-300 spectrometer. ¹H NMR spectra were obtained in (CD₃)₂SO and were referenced to TMS. Elemental analyses (CH) were performed by Galbraith Laboratories, Inc., Knoxville, TN, and are within ±0.4% of theory unless otherwise noted. Thin-layer chromatography was performed on Baker 1B-F silica gel plates.

Synthesis of 2,4-Diamino-5-(2-X-benzyl)pyrimidines. Most of the benzylpyrimidines in this study were synthesized by using the general procedure of Stenbuck et al. with minor variations on this theme.³² (See Scheme 2.) The following pyrimidines were synthesized by using commercially available or synthesized 2-X-benzaldehydes: such as X = 2-F, 2-Cl, 2-Br, 2-CH₃, 2-OCH₂CH₃, 2-OCH₂CH=CH₂, 2-O(CH₂)₃CH₃, 2-O(CH₂)₅CH₃, 2-OCH₂C₆H₅, 2,3-(OCH₃)₂, and 2,3,4-(OCH₃)₃. The general methodology (method A) is outlined as follows.

Method A: Synthesis of 2,4-Diamino-5-(2-bromobenzyl)pyrimidine (71). To a solution of sodium (2 g) in methanol (50 mL) were added 2-bromobenzaldehyde (9.8 g, 0.066 mol) and β-methoxypropionitrile (5.6 g, 0.066 mol). After heating at reflux temperature for 7 h, the solution was cooled, the methanol was removed under reduced pressure, and the mixture of benzal nitriles was dissolved in ether. The ethereal solution was washed consecutively by water (2 × 100 mL), NaHSO₃ (2 × 50 mL), and water (2 × 50 mL) and dried overnight (sodium sulfate). After removal of the drying agent and the solvent, the brown oil was distilled in vacuo. Weight of the mixture of benzal nitriles = 10.4 g (64%); bp = 160–176 °C/2.5 mmHg. Table 3 lists the benzal nitriles, III, obtained by this procedure. They were used in the next step without further purification.

A solution of guanidine hydrochloride (12 g, 0.126 mol) in methanol was neutralized by a methanolic solution of sodium (3 g, 0.130 mol). The mixture of benzal nitriles (10.4 g, 0.04 mol) was dissolved in the guanidine solution, and the resulting solution was refluxed for 24–48 h. After cooling the solvent was reduced in volume, and a precipitate was collected. The precipitate was further purified by passage through an alumina column and elution with an appropriate solvent (2–5% methanol in chloroform). The resulting solid, 2,4-diamino-5-

Table 3. Synthesis of α-(X-Benzylidene)-β-methoxypropionitriles III

method	X	yield (%)	bp (°C/mmHg)
A	2-F	61	123–140/1.4
A	2-Cl	65	136–152/1.3
A	2-Br	63	160–176/2.5
A	2-CH ₃	60	129–144/2.2
A	2-OCH ₂ CH ₃	51	130–153/2.2
A	2-O(CH ₂) ₃ CH ₃	36	155–169/0.4
A	2-O(CH ₂) ₅ CH ₃	49	142–164/0.2
A	2-OCH ₂ C ₆ H ₅	68	203–215/0.8
A	2-OCH ₂ CH=CH ₂	70	138–145/0.4
A	2,3-(OCH ₃) ₂	53	100–145/2.0
A	2,3,4-(OCH ₃) ₃	63	182–187/0.5

(2-bromobenzyl)pyrimidine, was recrystallized from absolute ethanol: mp 250–251 °C (EtOH), 40%; NMR (Me₂SO-*d*₆) δ 3.70 (s, 2, CH₂), 5.80 (s, 2, NH₂), 6.25 (s, 2, NH₂), 7.20 (m, 3, Ar), 7.35 (t, 1, Ar), 7.60 (s, 1, pyr C6–H). Anal. (C₁₁H₁₁N₄Br).

2,4-Diamino-5-(2-fluorobenzyl)pyrimidine (69): mp 181–182 °C (EtOH–benzene), 3%; NMR (Me₂SO-*d*₆) δ 3.62 (s, 2, CH₂), 5.80 (s, 2, NH₂), 6.22 (s, 2, NH₂), 7.20 (br-m, 4, Ar), 7.40 (d, 1, pyr C6–H). Anal. (C₁₁H₁₁N₄F).

2,4-Diamino-5-(2-chlorobenzyl)pyrimidine (70): mp 231–232 °C (EtOH), 39%; NMR (Me₂SO-*d*₆) δ 3.68 (s, 2, CH₂), 5.80 (s, 2, NH₂), 6.25 (s, 2, NH₂), 7.22 (br-m, 4, Ar), 7.45 (d, 1, pyr C6–H). Anal. (C₁₁H₁₁N₄Cl).

2,4-Diamino-5-(2-methylbenzyl)pyrimidine (73): mp 205–207 °C (EtOH–MeOH), 16%; NMR (Me₂SO-*d*₆) δ 2.20 (s, 3, CH₃), 3.58 (s, 2, CH₂), 5.90 (s, 2, NH₂), 6.35 (s, 2, NH₂), 7.15 (br-m, 4, Ar), 7.00 (m, 1, pyr C6–H). Anal. (C₁₂H₁₄N₄).

2,4-Diamino-5-(2-ethoxybenzyl)pyrimidine (79): mp 175–176 °C (EtOH), 4%; NMR (Me₂SO-*d*₆) δ 1.35 (t, 3, CH₃), 3.55 (s, 2, CH₂), 4.05 (q, 2, OCH₂), 5.80 (s, 2, NH₂), 6.20 (s, 2, NH₂), 7.00 (br-m, 4, Ar), 7.50 (s, 1, pyr C6–H). Anal. (C₁₃H₁₆N₄O).

2,4-Diamino-5-(2-propenyloxybenzyl)pyrimidine (80): mp 175–176 °C (MeOH–benzene), 9%; NMR (Me₂SO-*d*₆) δ 3.55 (s, 2, CH₂), 4.05 (d, 2, OCH₂), 5.35 (d, 1, =CH₂), 5.42 (d, 1, =CH₂), 5.70 (s, 2, NH₂), 6.10 (s, 2, NH₂), 6.05 (m, 1, CH), 6.85–7.18 (br-m, 4, Ar), 7.40 (s, 1, pyr C6–H). Anal. (C₁₄H₁₆N₄O).

2,4-Diamino-5-(2-butoxybenzyl)pyrimidine (81): mp 146–147 °C (EtOH–benzene), 5%; NMR (Me₂SO-*d*₆) δ 0.95 (t, 3, CH₃), 1.45 (m, 2, CH₂), 1.70 (m, 2, CH₂) 3.55 (s, 2, CH₂), 4.00 (t, 2, OCH₂), 5.70 (s, 2, NH₂), 6.10 (s, 2, NH₂), 6.85–7.20 (br-m, 4, Ar), 7.40 (s, 1, pyr C6–H). Anal. (C₁₅H₂₀N₄O).

2,4-Diamino-5-(2-hexyloxybenzyl)pyrimidine (82): mp 145–146 °C (EtOH), 2%; NMR (Me₂SO-*d*₆) δ 0.88 (t, 3, CH₃), 1.30 (m, 4, (CH₂)₂), 1.45 (m, 2, CH₂), 1.70 (m, 2, CH₂) 3.55 (s, 2, CH₂), 3.99 (t, 2, OCH₂), 5.70 (s, 2, NH₂), 6.10 (s, 2, NH₂), 6.85–7.20 (br-m, 4, Ar), 7.40 (s, 1, pyr C6–H). Anal. (C₁₇H₂₄N₄O).

2,4-Diamino-5-(2-benzyloxybenzyl)pyrimidine (83): mp 186–187 °C (MeOH–benzene), 7%; NMR (Me₂SO-*d*₆) δ 3.60 (s, 2, CH₂), 5.20 (s, 2, OCH₂), 5.73 (s, 2, NH₂), 6.10 (s, 2, NH₂),

6.90–7.20 (br-m, 4, Ar), 7.35 (s, 5, Ar), 7.40 (s, 1, pyr C6–H). Anal. (C₁₈H₁₈N₄O).

2,4-Diamino-5-(2,3-dimethoxybenzyl)pyrimidine (84): mp 194–195 °C (EtOH), 50%; NMR (Me₂SO-*d*₆) δ 3.50 (s, 2, CH₂), 3.68 (s, 3, OCH₃), 3.75 (s, 3, OCH₃), 5.70 (s, 2, NH₂), 6.10 (s, 2, NH₂), 6.62–6.95 (br-m, 3, Ar), 7.32 (s, 1, pyr C6–H). Anal. (C₁₃H₁₆N₄O₂).

2,4-Diamino-5-(2,3,4-trimethoxybenzyl)pyrimidine (Pseudo-TMP) (88): mp 221–223 °C (MeOH), 15%; NMR (Me₂SO-*d*₆) δ 3.40 (s, 2, CH₂), 3.70 (s, 9, OCH₃), 5.65 (s, 2, NH₂), 6.05 (s, 2, NH₂), 6.70 (br-m, 2, Ar), 7.30 (s, 1, pyr C6–H). Anal. (C₁₃H₁₆N₄O₂).

Method B: Synthesis of 2,4-Diamino-5-(2-hydroxybenzyl)pyrimidine (77). A solution of 2,4-diamino-5-(2-methoxybenzyl)pyrimidine (11.5 g, 0.05 mol) in 48% HBr (100 mL) was refluxed under nitrogen for 4 h. After cooling, the solvent was removed under reduced pressure to yield a red oil. The oil gradually solidified on standing to yield the hydrobromide salt of the desired pyrimidine. Recrystallization from ethanol yielded a pure solid: mp 271–273 °C (MeOH), 61%; NMR (Me₂SO-*d*₆) δ 3.50 (s, 2, CH₂), 6.70–6.85 (m, 2, Ar), 7.15 (m, 2, Ar), 7.30 (s, 1, pyr C6–H) 8.20 (s-br, 2, NH₂), 9.50 (s-br, 2, NH₂), 12.10 (s-br, 1, NH). Anal. (C₁₁H₁₂N₄·HBr).

Synthesis of 2,4-Diamino-5-(2-carboxamidomethoxybenzyl)pyrimidine (76). A suspension of potassium hydroxide (0.3 g, 0.005 mol) and 2,4-diamino-5-(2-hydroxybenzyl)pyrimidine (0.7 g, 0.003 mol) was heated at 70–80 °C for 30 min till solution ensued. Then chloroacetamide (0.6 g, 0.006 mol) was added and the solution heated at reflux for 20 h. The resulting suspension was filtered, and the gray solid was collected, recrystallized from water, and dried over P₂O₅: mp 207–209 °C (H₂O), 38%; NMR (Me₂SO-*d*₆) δ 3.35 (s, 2, NH₂), 3.60 (s, 2, CH₂), 4.30 (s, 2, OCH₂), 5.70 (s, 2, NH₂), 6.05 (s, 2, NH₂), 6.70–7.15 (br-m, 4, Ar), 7.40 (s, 1, pyr C6–H). Anal. (C₁₃H₁₅N₅O₂).

Synthesis of 2,4-Diamino-5-(2-(methylsulfonyloxy)benzyl)pyrimidine (75). A solution of 2,4-diamino-5-(2-hydroxybenzyl)pyrimidine (2.2 g, 0.01 mol) and 2 N KOH (15 mL) was cooled over ice. Methanesulfonyl chloride (1.4 g, 0.012 mol) was dissolved in 10 mL of benzene and added dropwise to the ice-cooled solution of the pyrimidine, with continuous agitation. After 10 min, a white precipitate was formed. It was collected, washed with 2 N KOH and water, and then recrystallized from ethanol: mp 203–204 °C (EtOH), 59%; NMR (Me₂SO-*d*₆) δ 3.50 (s, 3, CH₃), 3.65 (s, 2, CH₂), 5.75 (s, 2, NH₂), 6.10 (s, 2, NH₂), 7.10–7.30 (br-m, 4, Ar), 7.36 (s, 1, pyr C6–H). Anal. (C₁₂H₁₄N₄O₃S).

Method C: Synthesis of 2,4-Diamino-5-(2-iodobenzyl)pyrimidine (72). A solution of 2-iodobenzoic acid (31 g, 0.125 mol) in methanol was saturated with HCl gas and refluxed for 30 h. After removal of the methanol, the oil was dissolved in ether, washed successively with water (2 × 100 mL), 10% Na₂CO₃ (2 × 100 mL), and water (2 × 100 mL), and dried (MgSO₄). After removal of the ether the yellow oil was distilled to yield methyl 2-iodobenzoate: yield = 13 g (40%); bp = 92–93 °C (0.4 mmHg) (lit. bp 103.5 °C/1 mmHg).³³

To a solution of methyl 2-iodobenzoate (13 g, 0.05 mol) in toluene was added diisobutylaluminum hydride (60 mL of 1.0 M solution in toluene) at –60 °C. After 2 h the mixture was decomposed with excess saturated NH₄Cl solution, poured into an ice–water mixture, and extracted with ether. The ether extract was dried over MgSO₄ and evaporated to yield 2-iodobenzaldehyde: yield = 4 g (34%); mp = 38–40 °C (lit. mp = 39 °C).³⁴

To an ethanolic solution of sodium (2 g in 80 mL of ethanol) was added crude 2-iodobenzaldehyde (4.0 g, 0.017 mol) and β-methoxypropionitrile (1.6 g, 0.018 mol). The solution was refluxed for 24 h. Meanwhile a guanidine hydrochloride solution (5.0 g, 0.05 mol) was neutralized by an ethanolic solution of sodium (1.5 g in 50 mL of ethanol) and added to the flask. After continuous heating at reflux for another 48 h, the solution was washed, the ethanol removed, and the yellow precipitate recrystallized from ethanol to yield the desired pyrimidine: mp 266–267 °C (EtOH), 9%; NMR (Me₂

SO-*d*₆) δ 3.64 (s, 2, CH₂), 5.80 (s, 2, NH₂), 6.30 (s, 2, NH₂), 7.00–7.35 (br-m, 4, Ar), 7.90 (d, 1, pyr C6–H). Anal. (C₁₁H₁₁N₄I).

Method D: Synthesis of 2,4-Diamino-5-(2-methoxymethylbenzyl)pyrimidine (74). A solution of 2-(α-bromomethyl)benzotrile (15 g, 0.077 mol) in methanol (100 mL) was added dropwise to a solution of sodium (1.8 g) in methanol (100 mL). After refluxing for 5 h, the solution was washed, the solvent removed, and the oil extracted with ethyl acetate and washed with water. The ethyl acetate fractions were combined and dried overnight (MgSO₄). The solvent was removed and the resulting oil distilled to yield 2-(2-methoxymethyl)benzotrile: yield = 9.3 g (85%); bp = 80–85 °C/0.75 mmHg. The nitrile was used without further purification in the next step.

A mixture of Raney alloy (50; 50; 20 g), nitrile (9.3 g, 0.06 mol), and 50% v/v aqueous formic acid (300 mL) was refluxed for 36 h. After the mixture was filtered, the filtrate was diluted with water and extracted with ether. The ether extract was washed with NaHCO₃ (2 × 100 mL) and water (1 × 100 mL) and dried (MgSO₄). After removal of the ether a yellow solid was obtained which gave a positive test with 2,4-dinitrophenyl hydrazine: yield = 2.8 g (31%). The benzaldehyde was used without further purification.

The crude benzaldehyde (2.8 g, 0.018 mol), β-methoxypropionitrile (0.018 mol), and sodium (1 g) in methanol (150 mL) were refluxed for 20 h. Then a solution of guanidine hydrochloride (3.0 g, 0.03 mol) in sodium methoxide was added to the benzal nitrile solution, which was further refluxed for 48 h. After cooling the solvent was removed, and the yellow solid was decolorized with charcoal and recrystallized twice from ethanol to yield the desired pyrimidine: mp 205–206 °C (EtOH), 5%; NMR (Me₂SO-*d*₆) δ 3.20 (s, 3, CH₃), 3.50 (s, 2, CH₂), 4.40 (s, 2, CH₂O–), 5.70 (s, 2, NH₂), 6.10 (s, 2, NH₂), 7.00–7.30 (br-m, 4, Ar), 7.30 (m, 1, pyr C6–H). Anal. (C₁₃H₁₆N₄O).

Method E: Synthesis of 2,4-Diamino-5-(2-methoxybenzyl)pyrimidine (78). Derivatives synthesized by this method included the 2-OCH₃, 2,3-Cl₂, 2,4-Cl₂, and 2,4-(CH₃)₂ analogues. The general procedure of Poe et al. was used.³⁵ To a mixture of anisaldehyde (28 g, 0.2 mol), 3-anilinopropionitrile (38 g, 0.26 mol) and dimethyl sulfoxide (100 mL), which had been heated to 100 °C, was added a slurry of sodium methoxide (11 g, 0.20 mol) in dimethyl sulfoxide (60 mL). The temperature was raised to 125–130 °C. for 2 h. After cooling, the dark brown solution was poured into ice–water (1000 mL) and left overnight in the freezer. The slurry was filtered, and the gummy brown oil was triturated with cold ethanol–ether to yield a pale yellow product: yield = 38 g (72%); mp = 117–119 °C. Generally, the crude intermediates whose yields hovered between 36% and 50% were used without further purification in the next step.

Crude 2-methoxy-β-cyano-*N*-phenylcinnamylamine (26 g, 0.1 mol) was added to an ethanolic solution of guanidine (20 g of the hydrochloride neutralized by 5 g of sodium in 20 mL of ethanol). The solution was refluxed for 24 h. The ethanol was removed under reduced pressure, and the resulting orange oil was triturated with ethanol until a yellow solid appeared: mp 166–167 °C (EtOH), 50%; NMR (Me₂SO-*d*₆) δ 1.35 (t, 3, CH₃), 3.55 (s, 2, CH₂), 3.80 (s, 3, OCH₃), 5.75 (s, 2, NH₂), 6.12 (s, 2, NH₂), 7.10 (br-m, 4, Ar), 7.38 (s, 1, pyr C6–H). Anal. (C₁₂H₁₄N₄O).

2,4-Diamino-5-(2,3-dichlorobenzyl)pyrimidine (85): mp 268–270 °C (95% EtOH), 15%; NMR (Me₂SO-*d*₆) δ 3.70 (s, 2, CH₂), 5.80 (s, 2, NH₂), 6.20 (s, 2, NH₂), 7.00–7.21 (m, 2, Ar), 7.25 (s, 1, pyr C6–H), 7.45 (d, 1, Ar). Anal. (C₁₁H₁₀N₄Cl₂).

2,4-Diamino-5-(2,4-dichlorobenzyl)pyrimidine (87): mp 225–227 °C (MeOH–EtOH), 20%; NMR (Me₂SO-*d*₆) δ 3.60 (s, 2, CH₂), 5.75 (s, 2, NH₂), 6.20 (s, 2, NH₂), 7.10 (d, 1, Ar), 7.20 (s, 1, pyr C6–H), 7.30–7.55 (d, 2, Ar). Anal. (C₁₁H₁₀N₄Cl₂).

2,4-Diamino-5-(2,4-dimethylbenzyl)pyrimidine (86): mp 215–216 °C (EtOH), 62%; NMR (Me₂SO-*d*₆) δ 2.1 (s, 3, CH₃), 2.2 (s, 3, CH₃), 3.50 (s, 2, CH₂), 5.70 (s, 2, NH₂), 6.10 (s, 2,

Table 4. Synthesis of X-Benzaldehydes Using Method F

X	yield (%)	bp, °C (mmHg)	lit. bp, °C (mmHg)
2-O(CH ₂) ₃ CH ₃	46	90–93 (0.1)	105 (0.2)
2-O(CH ₂) ₅ CH ₃ ^a	75	144–146 (0.5)	
2-OCH ₂ C ₆ H ₅ ^b	57	49–50 (EtOH)	
2-OCH ₂ CH=CH ₂	59	105–108 (1.8)	136–138 (12)

^a Anal. (C₁₃H₁₈O₂) C, H. ^b Anal. (C₁₄H₁₂O₂) C, H.

NH₂), 6.80–6.90 (m, 3, Ar), 7.10 (s, 1, pyr C6–H), 7.45 (d, 1, Ar). Anal. (C₁₃H₁₆N₄).

Synthesis of *o*-Alkoxy-Substituted Benzaldehydes.

This general method was utilized for the synthesis of *o*-alkoxy-substituted benzaldehydes, which were not commercially available. (See Table 4.) Potassium hydroxide (11.2 g, 0.20 mol) was dissolved in a mixture of diglyme and ethanol and refluxed with salicylaldehyde (24.4 g, 0.2 mol) for 30 min. Then 1-bromobutane (27.4 g, 0.2 mol) was added, and the resulting solution was heated at reflux for 72 h. After cooling the potassium bromide was filtered off and the solvent removed under reduced pressure. The solid was washed with water and extracted with ether. The ethereal solution was washed successively by KOH (2 × 100 mL) and water (2 × 100 mL) and dried overnight (MgSO₄). After removal of the drying agent and solvent, the yellow oil was distilled to obtain the desired benzaldehyde. The following benzaldehydes were synthesized in this manner: 2-O(CH₂)₃CH₃;³⁶ 2-O(CH₂)₅CH₃;³⁷ 2-OCH₂C₆H₅ and 2-OCH₂CH=CH₂.³⁸

Acknowledgment. This research was funded in part by NIH Grant A132734-01 (C.S.) and NIH Grant RR-1081 (T. Ferrin, P.I.). Molecular graphics images were produced using the Midas Plus suite of programs at the UCSF Computer Graphics Laboratory.

Supporting Information Available: Tables of biological data and physical/chemical data (5 pages). Ordering information is given on any current masthead page.

References

- Hitchings, A. H. Selective Inhibitors Of Dihydrofolate Reductase (Nobel Lecture). *Angew. Chem., Int. Ed.* **1989**, 879–885.
- Kuyper, L. F. Inhibitors of Dihydrofolate Reductase. In *Computer Aided Drug Design. Methods and Applications*; Perun, T. J., Propst, C. L., Eds.; Marcel Dekker: New York, 1989; pp 327–370.
- Blaney, J. M.; Hansch, C.; Silipo, C.; Vittoria, A. Structure Activity Relationships of Dihydrofolate Reductase Inhibitors. *Chem. Rev.* **1984**, 84, 333–407.
- Selassie, C. D.; Klein, T. E. Comparative Quantitative Structure Activity Relationships of the Inhibition of Dihydrofolate Reductase. In *Comparative Quantitative Structure Activity Relationships*; Devillers, J., Ed.; Taylor and Francis: Washington, DC, 1998; in press.
- Selassie, C. D.; Fang, Z. X.; Li, R. L.; Hansch, C.; Debnath, G.; Klein, T. E.; Langridge, R.; Kaufman, B. T. On the Structure Selectivity Problem in Drug Design. A Comparative Study of Benzylpyrimidine Inhibition of Vertebrate and Bacterial Dihydrofolate Reductase via Molecular Graphics and Quantitative Structure Activity Relationships. *J. Med. Chem.* **1989**, 32, 1895–1905.
- Selassie, C. D.; Klein, T. E. Building Bridges: QSAR and Molecular Graphics. In *3D Drug Design: Theory, Methods and Applications*; Kubinyi, H., Ed.; Escom Science Publishers: Leiden, 1993; pp 256–275.
- Cheung, H. T. A.; Searle, M. S.; Feeney, J.; Birdsall, B.; Roberts, G. C. K.; Kompis, I.; Hammond, S. J. Trimethoprim Binding to *Lactobacillus casei* Dihydrofolate Reductase: A ¹³C NMR study using Selectively ¹³C-enriched Trimethoprim. *Biochemistry* **1986**, 25, 1925–1931.
- Kubinyi, H.; Kehrhn, O. Quantitative Structure Activity Relationships. VI. Nonlinear Dependence of Biological Activity on Hydrophobic Character: Calculation Procedures for the Bilinear Model. *Arzneim-Forsch. (Drug Res.)* **1978**, 28, 598–601.
- Selassie, C. D.; Li, R. L.; Poe, M.; Hansch, C. On the Optimization of Hydrophobic and Hydrophilic Substituent Interactions of 2,4-diamino-5-(substituted benzyl) Pyrimidines with Dihydrofolate Reductase. *J. Med. Chem.* **1991**, 34, 46–54.

- Stammers, D. K.; Champness, J. N.; Beddell, C. R.; Dann, J. G.; Eliopoulos, E.; Geddes, A. J.; Ogg, D.; North, A. C. T. The Structure of Mouse L1210 Dihydrofolate Reductase-Drug Complexes and the Construction of a Model of Human Enzyme. *FEBS Lett.* **1987**, 218, 178–184.
- Volz, K. W.; Matthews, D. A.; Alden, R. A.; Freer, S. T.; Hansch, C.; Kaufman, B. T.; Kraut, J. Crystal Structure of Avian Dihydrofolate Reductase Containing Phenyltriazine and NADPH. *J. Biol. Chem.* **1982**, 257, 2528–2536.
- Hansch, C.; Leo, A. Steric Effects on Organic Reactions. In *Exploring QSAR: Fundamentals and Applications in Chemistry and Biology*; Heller, S. R., Ed.; American Chemical Society: Washington, DC, 1995; p 76.
- Stuart, A.; Paterson, T.; Roth, B.; Aig, E. 2,4-Diamino-5-benzylpyrimidines and Analogues as Antibacterial Agents. 6. A One Step Synthesis of New Trimethoprim Derivatives and Activity Analysis by Molecular Modeling. *J. Med. Chem.* **1983**, 26, 607–673.
- Fleischman, S. H.; Brooks, C. L., III. Protein-Drug Interactions: Characterization of Inhibitor Binding in Complexes of DHFR with Trimethoprim and Related Derivatives. *Proteins* **1990**, 7, 52–61.
- McDonald, J. J.; Brooks, C. L., III. Theoretical Approach to Drug Design. 2. Relative Thermodynamics of Inhibitor Binding by Chicken Dihydrofolate Reductase to Ethyl Derivatives of Trimethoprim Substituted at 3', 4', and 4'-positions. *J. Am. Chem. Soc.* **1991**, 113, 2295–2301.
- Li, R. L.; Hansch, C.; Matthews, D.; Blaney, J. M.; Langridge, R.; Delcamp, T. J.; Susten, S. S.; Freisheim, J. H. A Comparison by QSAR, Crystallography and Computer Graphics of the Inhibition of Various Dihydrofolate Reductases by 5-(X-Benzyl)-2,4-diamino Pyrimidines. *Quant. Struct. Act. Relat.* **1982**, 1, 1–7.
- Pearlman, D. A.; Case, D. A.; Caldwell, J. W.; Ross, W. S.; Cheatham, T. C.; Debolt, S. E.; Ferguson, D. M.; Siebel, G. L.; Kollman, P. A. AMBER, A Package of Computer Programs for Applying Molecular Mechanics, Molecular Dynamics and Free Energy Calculations to Simulate the Structural and Energetic Properties of Molecules. *Computer Phys. Commun.* **1995**, 91, 1–41.
- Huang, C. C.; Couch, A. S.; Patterson, E. F.; Ferrin, T. E. MidasPlus Release 2.0, 1994.
- Matthews, D. A.; Bolin, J. T.; Burrige, J. M.; Filman, D. J.; Volz, K. W.; Kaufman, B. T.; Beddell, C. R.; Champness, J. N.; Stammers, D. K.; Kraut, J. Refined Structures of *E. coli* and Chicken Liver DHFR Containing Bound Trimethoprim. *J. Biol. Chem.* **1985**, 260, 381–391.
- Feeney, J. NMR Studies of Interactions of Ligands with Dihydrofolate Reductase. *Biochem. Pharmacol.* **1990**, 40, 141–152.
- Searle, M. S.; Forster, M. J.; Birdsall, B.; Roberts, G. C. K.; Feeney, J.; Cheng, H. T. A.; Kompis, I.; Geddes, A. J. Dynamics of Trimethoprim Bond to Dihydrofolate Reductase. *Proc. Natl. Acad. Sci. U.S.A.* **1988**, 85, 3787–3791.
- Blakely, R. L.; Piper, J. R.; Mahorag, G.; Appleman, J. R.; Delcamp, T. J.; Freisheim, J. H.; Kulinski, R. F.; Montgomery, J. Mobility of the Spin-Labeled Side Chains of Some Novel Antifolate Inhibitors in their Complexes with Dihydrofolate Reductase. *Eur. J. Biochem.* **1991**, 196, 271–280.
- Stammers, D. K.; Champness, J. N.; Dann, J. G.; Beddell, C. R. The Three-Dimensional Structure of Mouse L1210 Dihydrofolate Reductase. In *Chemistry and Biology of Pteridines*; Blair, J. A., Ed.; Walter de Gruyter: New York, 1983; pp 567–57.
- Koetzle, T. F.; Williams, G. J. B. The Crystal and Molecular Structure of the Antifolate Drug Trimethoprim (2,4-diamino-5-(3,4,5-Trimethoxybenzyl) Pyrimidine). A Neutron Diffraction Study. *J. Am. Chem. Soc.* **1976**, 98, 2074–2078.
- Brossi, A.; Sharma, P. N.; Takahashi, K.; Chiang, J. F.; Karle, I. L.; Seibert, G. Tetramethoprim and Pentamethoprim: Synthesis Antibacterial Properties and X-ray Structures. *Helv. Chim. Acta* **1983**, 66, 795–800.
- Roth, B.; Rauckman, B. S.; Ferone, R.; Bacanari, D. P.; Champness, J. N.; Hyde, R. M. 2,4-Diamino-5-benzylpyrimidines as Antibacterial Agents. 7. Analysis of the Effect of 3,5-dialkyl Substituent Size And Shape On Binding to Four Different Dihydrofolate Reductase Enzymes. *J. Med. Chem.* **1987**, 30, 348–356.
- Chan, J. H.; Roth, B. 2,4-Diamino-5-benzylpyrimidines as Antibacterial Agents. 14. 2,3-Dihydro-1-(2,4-diamino-5-pyrimidyl)-1H-Indenes as Conformationally Restricted Analogues of Trimethoprim. *J. Med. Chem.* **1991**, 34, 550–555.
- Selassie, C.; Gan, W. X.; Yi, C.; Liu, M. Unpublished observations.
- Roberts, G. C. K. Understanding the Specificity of the Dihydrofolate Reductase Binding Site. *NATO ASI Ser., Ser. A* **1989**, 183, 209–220.
- Hansch, C.; Leo, A.; Hoekman, D. Hammett Sigmas. In *Exploring QSAR: Hydrophobic, Electronic and Steric Constants*; Heller, S. R., Ed.; American Chemical Society: Washington, DC, 1995; pp 217–304.

- (31) Dietrich, S. W.; Blaney, J. M.; Reynolds, M. A.; Jow, P. Y. C.; Hansch, C. Quantitative Structure Selectivity Relationships. Comparison of the Inhibition of *Escherichia coli* and Bovine Liver Dihydrofolate Reductase by 5-(substituted benzyl)-2,4-diamino Pyrimidines. *J. Med. Chem.* **1980**, *23*, 1205–1212.
- (32) Stenbuck, P.; Baltzly, R.; Hood, H. M. A New Synthesis of 5-benzyl Pyrimidines. *J. Org. Chem.* **1963**, *28*, 1983–1988.
- (33) Brown, H. C.; Okamoto, Y.; Ham, G. The Effect of Halogen Substituents Upon the Rates of Electrophilic Reactions. *J. Am. Chem. Soc.* **1957**, *79*, 1906–1909.
- (34) *The Systematic Identification of Organic Compounds. A Laboratory Manual*, 6th ed.; Shriner, R. L., Fuson, R. C., Curtin, D. Y., Morrill, T. C., Eds.; John Wiley & Sons: New York, 1980; p 538.
- (35) Poe, M.; Ruyle, W. V. Inhibitor of Dihydrofolate Reductase. U.S. Patent 4,258,405, 1981.
- (36) Katz, L.; Karger, L.; Schroeder, W.; Cohen, M. Hydrazine Derivatives. I. Benzalthio and Bisbenzaldithio-Salicyl Hydrazides. *J. Org. Chem.* **1953**, *18*, 1380–1402.
- (37) Coates, L. V.; Drain, D. J.; McCrae, F. J. The Preparation and Evaluation of Some Phenolic Ethers as Antifungal Agents. *J. Pharm. Pharmacol.* **1959**, *11*, 240T–249T.
- (38) Pansevich-Kolyada, V. I.; Strel'tsov, A. E. Ethers with an Allylic Double Bond. VII. Allyl Ether of Salicylaldehyde in the Grignard Reaction. *Zh. Obshchei. Khim.* **1960**, *30*, 3261–3263.

JM970776J